Study on Thermal Enhancement Mechanism of POSS-Containing Hybrid Nanocomposites and Relationship Between Thermal Properties and their Molecular Structure

Yan Feng,[1,2] Yong Jia,[2] Shanyi Guang,[1] Hongyao Xu[1,2]

[1]*College of Material Science and Engineering, State Key Laboratory for Modification of Chemical Fibers and Polymeric Materials, Donghua University, Shanghai 201620, People's Republic of China*
[2]*School of Chemistry and Chemical Engineering, Anhui University, Hefei 230039, People's Republic of China*

Received 9 June 2009; accepted 18 August 2009
DOI 10.1002/app.31319
Published online 7 October 2009 in Wiley InterScience (www.interscience.wiley.com).

ABSTRACT: In this study, a series of poly(4-acetoxystyrene) (PAS)-octavinyl polyhedral oligomeric silsesquioxane (POSS) blends and the polystyrene (PS)-octavinyl POSS blends were prepared by the solution-blending method and characterized with Fourier transform infrared (FTIR), X-ray diffraction (XRD), transmission electron microscopy (TEM), differential scanning calorimetry (DSC), and thermogravimetric analysis (TGA) techniques. The results show that the glass-transition temperature (T_g) of the PAS-POSS blends increases at a relatively low POSS content and then decreases at a relatively high POSS content. POSS can effectively improve the thermal stability of the PAS-POSS blends at low POSS content, and T_g of PAS-POSS blends decreases with the increase in POSS content at relatively high POSS content. However, the T_g of the PS-POSS blends persistently decreases even at very low POSS content. T_g change mechanism was investigated in detail by XRD, TEM, and FTIR spectra. The influence mechanism of POSS content and dispersion in composites, and parent polymer structure on thermal properties of the blends was investigated in detail.
 J Appl Polym Sci 115: 2212–2220, 2010

Key words: octavinyl polyhedral oligomeric silsesquioxane; blends; thermal properties

INTRODUCTION

Amorphous polymers such as poly(4-acetoxystyrene) (PAS), polystyrene (PS), and poly(methyl methacrylate) (PMMA), are very attractive for many engineering applications because of their excellent transparencies, high moduli, and relative ease of processing. However, their low glass-transition temperatures (T_g) and relatively poor thermal stabilities limited their further application in several situations, such as optical electronic industry, including compact disks, optical glass, and optical fibers. A good way to solve this problem is to develop organic/inorganic composites by incorporating an inorganic fraction, particularly nanometer particles, into the polymeric matrix by physical blending.[1–10] The resulting composites often show obvious improvement in thermal and mechanical properties compared with the parent polymers. However, the enhancement mechanism so far has not been understood completely.

Polyhedral oligomeric silsesquioxane (POSS) is a type of nanoscale molecule that has a well-defined cube-like inorganic core (Si_8O_{12}) with eight organic functional groups (reactive or inert).[11] It is an inner inorganic–organic hybrid system at the molecular level, and it can be easily dispersed into polymer uniformly as inorganic particles without further surface modification. Therefore, some researchers have shifted their interests toward the polymer/POSS hybrid nanocomposites, which can be simply prepared by blending inorganic POSS with organic polymer effectively, and a wide variety of studies have been carried out to probe their thermal properties,[12–20] morphology,[12,13,16,20] mechanical characteristics,[19,21–24] and self-assembly.[12,25,26]

In our previous research, a series of PMMA-octavinyl POSS blends were prepared by the solution-blending method. Differential scanning calorimetry (DSC) and thermogravimetric analysis (TGA) measurements revealed that the incorporation of POSS into polymers can improve the thermal properties of polymeric materials. The Fourier transform infrared (FTIR) spectra, X-ray diffraction (XRD) patterns, and

Correspondence to: H. Xu (hongyaoxu@163.com).
Contract grant sponsor: National Natural Science Fund of China; contract grant numbers: 90606011, 50472038.
Contract grant sponsor: Ph.D. Program Foundation of Ministry of Education of China; contract grant number: 20070255012.
Contract grant sponsor: Shanghai Leading Academic Discipline Project; contract grant number: B603.
Contract grant sponsor: Program of Introducing Talents of Discipline to Universities; contract grant number: 111-2-04.

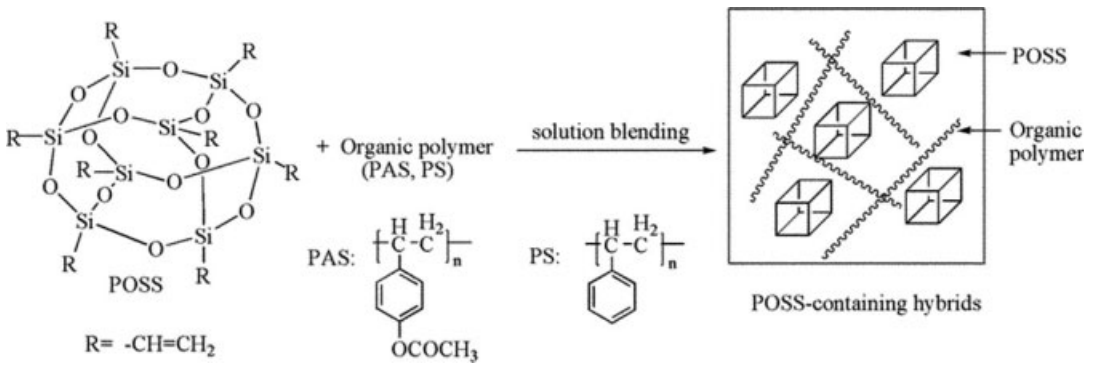

Scheme 1 Preparation route of POSS-containing hybrid nanocomposites.

transmission electron microscopy (TEM) photographs were used to explain the T_g improvement mechanism.[27] In this article, for further studying on the thermal enhancement mechanism of POSS-containing hybrid nanocomposites and the relationship between thermal properties and their molecular structure, we chose two polymers (PAS and PS), which have the similar molecular structure and different molecular polarity, prepared a series of poly(4-acetoxystyrene)-octavinyl polyhedral oligomeric silsesquioxane (PAS-POSS) and polystyrene-octavinyl polyhedral oligomeric silsesquioxane (PS-POSS) blends containing various POSS content, characterized their thermal properties, and further investigated the influence mechanism of parent polymer molecular structure, and POSS content and dispersion in composites on thermal properties of hybrid composites.

EXPERIMENTAL

Materials

Octavinyl POSS monomers were synthesized according to the procedures described in Ref. 28. 4-Acetoxystyrene and styrene were purchased from Aldrich (St. Louis, MO), distilled from calcium hydride under reduced pressure before use, and stored in sealed ampoules in a refrigerator. Azobis-(isobutyronitrile) (AIBN), purchased from Shanghai Chemical Reagent Co. (Shanghai, China), was refined in heated ethanol and kept in a dried box. Tetrahydrofuran (THF) and 1,4-dioxane, also purchased from Shanghai Chemical Reagent Co., were dried over 4 Å molecular sieves and distilled from sodium benzophenone ketyl immediately before use. All other solvents were used as received.

Polymerization

The polymerization reactions were carried out under nitrogen protection with a vacuum-line system. The polymers used in this study, PAS and PS, were synthesized by free-radical polymerization in 1,4-dioxane at 70°C under a nitrogen atmosphere with AIBN as the initiator for 8 h. The PAS was purified by dissolution in THF, reprecipitation from petroleum ether, and then drying in a vacuum oven at 30°C for 12 h. The PS was reprecipitated from methanol, other manipulations were similar to the PAS. The results of GPC show PAS has a weight-average molecular weight (M_w) of 13,500 g/mol and a polydispersity index [PDI; i.e., weight-average molecular weight/number-average molecular weight (M_w/M_n)] of 1.44, and the polymerization of styrene results in a M_w of 12, 800 g/mol and PDI of 1.88.

Preparation of composites

The composites were prepared with solution-blending method by dissolution of PAS or PS and POSS in THF at room temperature (Scheme 1). In a typical process, 9.916 mmol of PAS and 0.084 mmol of POSS monomer were dissolved in 10 mL THF and stirred for 30 min. The solution was allowed to evaporate slowly at 25°C for 24 h on a Teflon plate and dried in a vacuum oven at 60°C to a constant weight to ensure total elimination of the solvent. The dried films were then ground into powders.

Instrumentation

FTIR spectra were measured with a spectral resolution of 1 cm^{-1} on a Nicolet Avatar 320 FTIR spectrophotometer (Nicolet Analytical Instruments, Madison, WI) in transmission mode with KBr disks at room temperature. M_w, M_n, and PDI were determined by a Waters 510 gel permeation chromatograph (Waters Chromatography Division, Millipore Corp., Milford, MA). DSC was performed on a DSC 9000 (Dupont, Boston, MA) equipped with a liquid nitrogen cooling accessory unit under a continuous nitrogen purge (50 mL/min). The first scan rate was 20°C/min within the temperature range 20–130°C. The sample was quickly cooled to 0°C after the first

scan, and it was subsequently reheated from 20 to 250°C at 10°C/min. T_g was taken as the midpoint of the specific heat increment. TGA was carried out using a TGA 2050 thermogravimetric analyzer (TA Instruments, New Castle, DE) with a heating rate of 20°C/min from 25 to 700°C under a continuous nitrogen purge (100 mL/min). The thermal degradation temperature (T_d) was defined as the temperature of 10% weight loss. XRD data were recorded using a Bruker AXS D8 Discover instrument (Bruker-AXS GmbH, Karlsruhe, Germany) with a general area detector diffraction system powder diffractometer and a charged coupling device camera detector. CuKα radiation was generated at 40 kV and 40 mA. TEM micrographs were obtained with a JEM-100SX instrument (Jeol Ltd., Tokyo, Japan) operated at 100 kV. The specimens were embedded in an epoxy resin, and ultrathin sections (~ 60 nm) were cut and examined.

RESULTS AND DISCUSSION

FTIR spectra

FTIR was used to check the structures of the resulting PAS-POSS and PS-POSS blends. Figure 1(a) shows the FTIR spectra of PAS-POSS blends as well as pure POSS and PAS for comparison. The pure POSS shows a strong and symmetric Si—O—Si stretching absorption band at ~ 1109 cm^{-1}, which is the characteristic absorption peak of silsesquioxane cages. The PAS shows two characteristic absorptions at 1763 and 1216 cm^{-1}, which are assigned as the carbonyl stretching vibration and the strong Ph—O stretching absorption, respectively. The peak at ~ 1500 cm^{-1} comes from the skeletal vibration of aromatic rings. The stretching absorption bands of methylene and methine groups are located at ~ 2900 cm^{-1}. The *para*-substituted aromatic ring shows the characteristic peaks at 910 and 848 cm^{-1}, which are assigned as two out-of-plane bending δs (C—H). The IR spectra of the PAS-POSS blends [Fig. 1(a)] is very similar to that of the PAS except that a sharp and strong Si—O—Si stretching peak appear at 1109 cm^{-1} in all PAS-POSS blends. Analogical phenomenon was found in the IR spectra of the PS-POSS blends [Fig. 1(b)]. The PS shows two characteristic out-of-plane wagging absorption bands of single-substituted aromatic ring at 699 and 756 cm^{-1}. The peaks at ~ 1500 cm^{-1} are assigned to the skeletal vibration of aromatic ring. The stretching absorption bands of methylene and methine groups are located at ~ 2900 cm^{-1}. The spectra of all PS-POSS nanocomposites are similar to that of the PS, except that a strong and symmetric peak appears at ~ 1109 cm^{-1} in all the spectra, which is the characteristic Si—O—Si stretching of silsesquioxane cages. The consistent presence of this Si—O—Si stretching peak at 1109 cm^{-1} confirms that the POSS cage is truly present in the resulting hybrid nanocomposites.

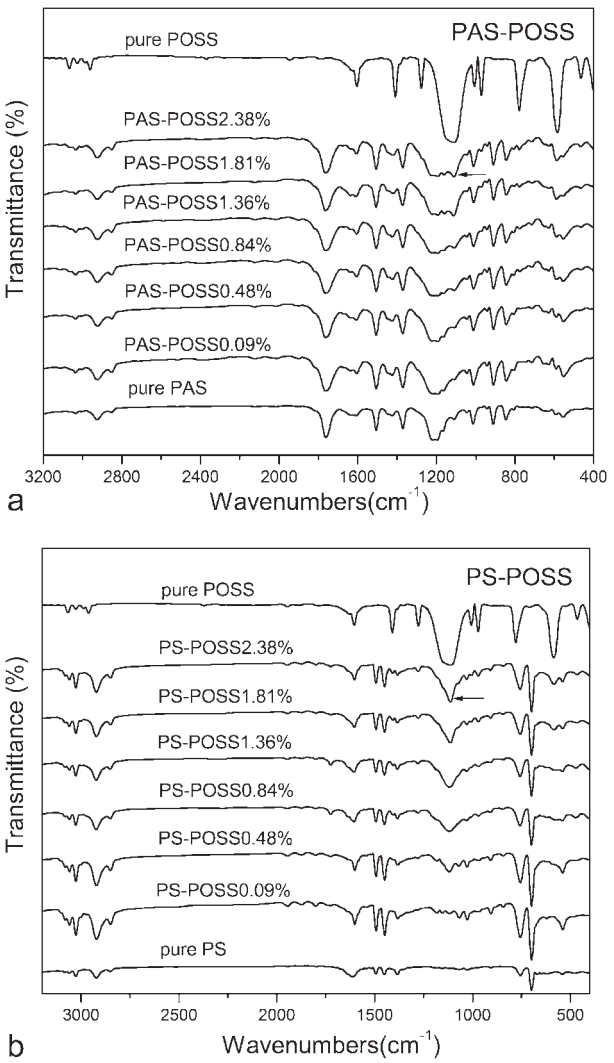

Figure 1 (a) FTIR spectra of pure POSS, PAS, and PAS-POSS blends. (b) FTIR spectra of pure POSS, PS, and PS-POSS blends.

DSC and TGA thermograms

The DSC and TGA techniques were used to investigate the thermal properties of the PAS-POSS and PS-POSS blends. Figure 2(a) shows the DSC thermograms of PAS and PAS-POSS blends and Table I shows their thermal properties. The PAS homopolymer has a T_g at 110.4°C. When 0.09 mol % POSS was incorporated into the PAS polymers, T_g slightly increased to 116.5°C. When 0.48 mol % POSS was blended into the PAS polymers, T_g further increased to 120.8°C. This proves that the incorporation of a relatively small amount of POSS macromers into homopolymers can effectively improve the T_g of the mother polymers. However, the T_g of the PAS-POSS

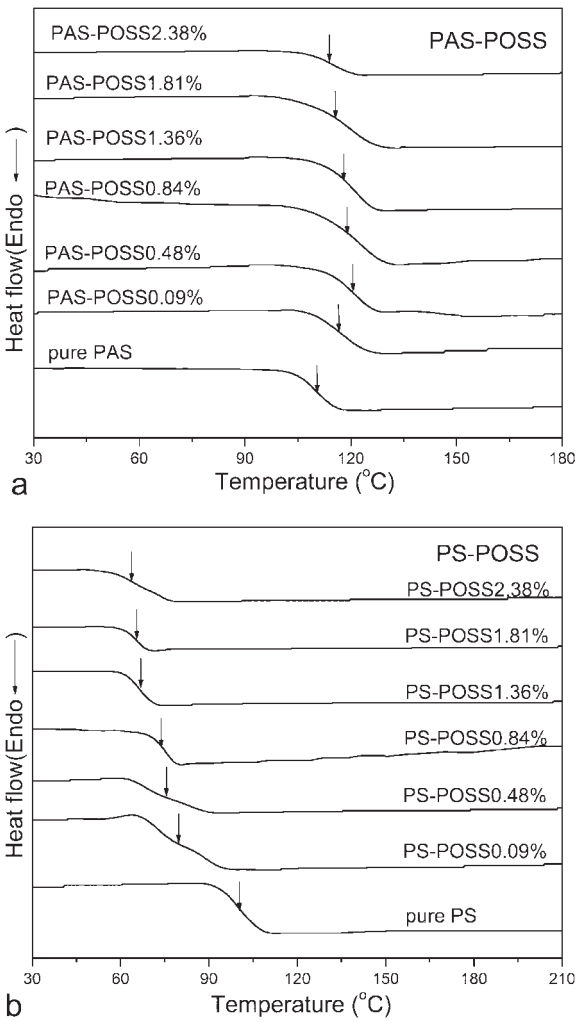

Figure 2 (a) DSC thermograms of PAS and PAS-POSS blends. (b) DSC thermograms of PS and PS-POSS blends.

blends displayed a decrease tendency with further increase in the POSS content. For example, when 0.84 mol % POSS was blended into the PAS system, the T_g at 118.7°C was observed, which is lower than that of PAS-POSS 0.48%, but still 8.3°C higher than that of the mother PAS. When the molar percentage of POSS in the hybrid reached 2.38%, the PAS-POSS blends showed a lower T_g at 113.9°C. As a result, the observed T_g of the PAS-POSS blends shows a tendency of first increasing and then decreasing with the increase in the POSS content, which is similar to our previous research for PMMA-POSS blends.[27] The T_g of the PAS-POSS blends is always higher than that of the parent homopolymer in our experiments and shows the better thermal properties than the mother PAS.

For comparison, Figure 2(b) shows the DSC thermograms of PS and various PS-POSS blends and their thermal properties were also showed in Table I. The PS homopolymer has a T_g at 100.6°C. When 0.09 mol % POSS was incorporated into the PS polymers, different from PAS-POSS blends, the PS-POSS 0.09% shows a T_g at 80.1°C, which is below that of parent PS, and it is found that the T_g of PS-POSS blends further decreases with the increase in POSS content. The results show the PS-POSS blends have the poor thermal properties and the T_g of the PS-POSS blends is always lower than that of neat PS in our experiments.

Analyzing the structure of the mother polymer, it is found that the PAS has the polar carbonyl group in its molecule structure and the PS has none. The polarity of the group in the polymer can influence the interaction between polymer and POSS, and further work on the thermal properties of hybrid nanocomposites. The dipole–dipole interaction between POSS and polymer in the PAS-POSS blends is much stronger than that of the PS-POSS blends, which will possibly be the reason that, the T_g of the PAS-POSS blends appears an increase tendency compared with the mother PAS at a relatively low POSS content. The similar results were found in our previous research for PMMA-POSS blends.[27] On the contrary, the weak polar polymer mixed with POSS to prepare the hybrid blend, which often results in low T_g. For

TABLE I
Thermal Properties of the PAS-POSS and PS-POSS Blends

PAS-POSS					PS-POSS				
POSS content (mol %)	POSS content (wt %)	T_g[a] (°C)	T_d[b] (°C)	Char yield[c] (%)	POSS content (mol %)	POSS content (wt %)	T_g[a] (°C)	T_d[b] (°C)	Char yield[c] (%)
0.00	0.00	110.4	378.9	4.8	0.00	0.00	100.6	346.5	0.43
0.09	0.34	116.5	395.9	4.8	0.09	0.54	80.1	365.2	0.85
0.48	1.84	120.8	401.0	7.3	0.48	2.84	75.5	376.8	3.06
0.84	3.20	118.7	376.8	11.9	0.84	4.90	73.9	309.5	6.79
1.36	5.10	117.9	373.6	15.7	1.36	7.73	66.9	313.5	9.36
1.81	6.71	115.0	377.2	15.5	1.81	10.07	65.5	347.7	6.82
2.38	8.68	113.9	376.1	17.2	2.38	12.90	63.7	326.2	10.56

[a] The data were gathered by DSC during the second melt with a heating rate of 10°C/min.
[b] The data were determined by TGA at the temperature of 10% weight loss.
[c] The data were the char residues based on the TGA curve at 500°C.

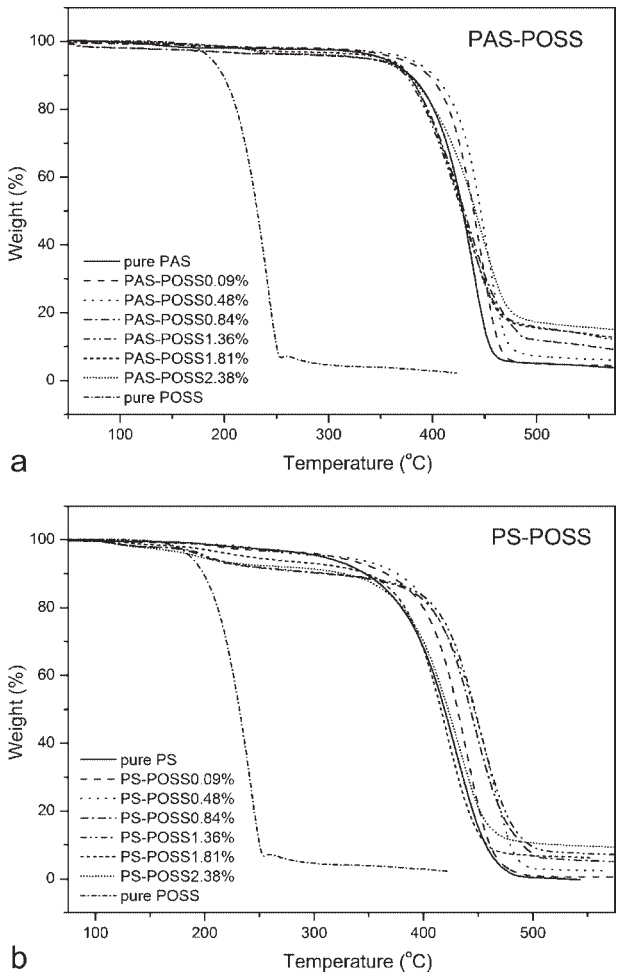

Figure 3 (a) TGA thermograms of POSS, PAS, and PAS-POSS blends. (b) TGA thermograms of POSS, PS, and PS-POSS blends.

example, the T_g of the PS-POSS blends is always lower than that of the neat PS, suggesting that the polarity or structure of polymers also yields important influence on thermal properties of hybrid nanocomposites.

Figure 3(a) shows the TGA thermograms of various PAS-POSS blends, pure POSS and pure PAS. POSS does sublime between 200 and 250°C. The pure PAS has a T_d at 378.9°C and has 4.8% char yield when the temperature reaches 500°C. For PAS-POSS blends, the T_d and char yield increase with the increase in POSS content when the molar percentage of POSS in the hybrids is 0.48% or lower. For example, PAS-POSS0.48% has a T_d at 401.0°C (22.1°C higher than pure PAS) and 7.3% char yield at 500°C. When the molar percentage of POSS in the hybrids reaches 0.84%, the T_d shows a decrease tendency but char yield still increases with the increase in POSS content. Interestingly, the similar change phenomenon has also been observed in the PS-POSS blends [Fig. 3(b)]. When the molar percentage of POSS is 0.48% or lower in the PS-POSS blends, the T_d and char yield increase with the increase in POSS content and when the molar percentage of POSS in the hybrids reaches 0.84%, the T_d shows a decrease tendency but char yield still increases with the increase in POSS content. These facts indicate that the low-content POSS can effectively improve the thermal stability of the POSS-based hybrid nanocomposites. The heat degradation has been restrained remarkably at the low POSS content in hybrids, which makes the hybrids possess potential application as flame retardant.

T_g change mechanism

In our previous study, we have reported the pendent poly(vinylpyrrolidone-*co*-isobutylstyryl-POSS) (PVP-*co*-POSS), the star poly(acetoxystyrene-*co*-octavinyl-POSS) (PAS-*co*-POSS) and poly(styrene-*co*-octavinyl-POSS) (PS-*co*-POSS) hybrid nanocomposites that are synthesized by radical polymerization.[29–31] The POSS molecules in these nonocomposites are covalently bonded to the polymer and dispersed uniformly in the nanocomposites at molecular level. The DSC and TGA measurements reveal that the incorporation of POSS into polymers can improve the thermal properties of polymeric materials. The T_g of these nanocomposites from single functional POSS shows a first decrease and then increase tendency with the increase in the POSS content,[29] in which, at low POSS content POSS dilute effect is the main factor, and at relatively high POSS content dipole–dipole interaction between POSS and polymer, and hindrance effect of nanosize POSS to motion of PVP molecular chain play more important role. The nanocomposites from multifunctional POSS show T_g enhancement and high-thermal stability even at very low POSS content, which are originated from crosslink hybrid structure, dipole–dipole interaction between polymer and POSS, and polymeric chain motion hindrance from nanosized inorganic POSS core.[31] In this study, the T_g values of PAS-POSS blends exhibit a first increase and then decrease tendency with the increase in POSS content and the T_g values of PS-POSS blends always decrease with the increase in POSS content. Except for the influence of the polarity of polymer, the dispersion of POSS in the nanocomposites may be one of the important reasons that lead to the T_g change for the hybrid materials. To further verify this hypothesis, XRD and TEM were used to characterize the miscibility of the PAS-POSS blends.

XRD patterns

XRD was used to further characterize the dispersion of POSS of the PAS-POSS blends. Diffraction patterns for the pure PAS, POSS, and the PAS-POSS

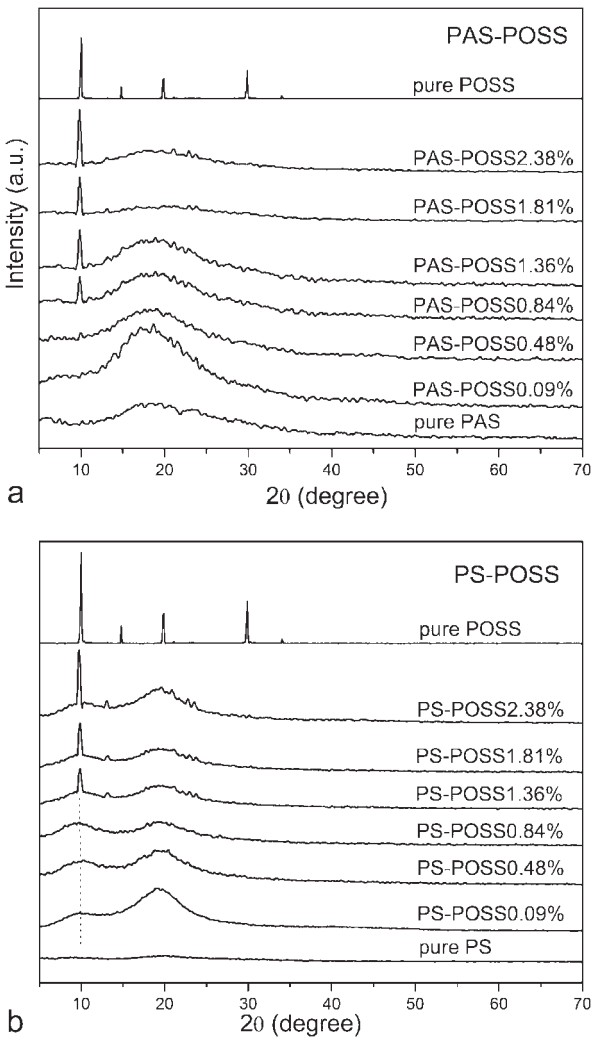

Figure 4 (a) XRD patterns of POSS, PAS, and PAS-POSS blends. (b) XRD patterns of POSS, PS, and PS-POSS blends.

blends are shown in Figure 4(a). The X-ray powder pattern of POSS shows three main characteristic diffraction peaks at 9.8°, 20.1°, and 29.9° (2θ). These values are typical for the crystal structure of the POSS. A broad amorphous diffraction peak of PAS is at ~ 17° (2θ). In each case, diffraction patterns of the PAS-POSS blends with 0.09 mol % and 0.48 mol % POSS have only a broad amorphous peak at ~ 17° (2θ), corresponding to the amorphous PAS matrix peak. The appearance of this broad amorphous peak means that no significant aggregation happens when the molar percentage of POSS is 0.48% or lower, and the PAS and POSS are relatively distributed evenly in the nanocomposites and the nanosize POSS can hinder the motion of PAS molecular chain and make a contribution to the T_g increase. When the POSS molar percentage reaches 0.84%, a new peak matching the peak of the POSS at 9.8° (2θ) appears and becomes more prominent at PAS-POSS 1.36%. The appearance of this characteristic diffraction peak in the PAS-POSS blend shows the POSS nanoparticles have aggregated in the blend and the degree of aggregation increases with the further increase in the POSS content. The aggregated POSS cluster results in the T_g decrease. Similar aggregation phenomenon was also found in PS-POSS blends when the molar percentage of POSS is 1.36% [Fig. 4(b)].

An analysis of XRD patterns of the PAS-POSS blend systems shows that significant aggregation of the POSS becomes apparent when the molar percentage of POSS reaches 0.84%. In combination with the DSC results, we can realize that the dispersion of POSS nanoparticles in the PAS-POSS blends shows an obvious effect on the thermal properties of nanocomposites. At a relatively low POSS content (<0.84 mol %), the POSS nanoparticles can be relatively distributed uniformly in the nanocomposites, resulting in an increase in T_g. At a relatively high POSS content (>0.84 mol %), the aggregation becomes dominant and leads to a decrease of T_g. The results accord with that of DSC ones well. For PS-POSS blends, the T_g values persistently decrease with the increase in POSS content even when the POSS was mixed into the PS matrix uniformly at the low POSS content. The absence of strong dipole–dipole interaction between POSS and polymer in the PS-POSS blends may be the main reason to result in the low T_g.

TEM analysis

Although the XRD data indicate the aggregation of POSS nanoparticles in PAS-POSS blends at the higher POSS content, this does not unambiguously prove the nanoscale morphology formed by POSS particles. As a result, the PAS-POSS blends at three different POSS molar contents were characterized by TEM to investigate possible aggregation at the higher POSS content. The sample was not stained because the electron density differences between POSS core (higher electron density due to the presence of silicon atoms) and organic PAS chains should produce sufficient contrast to observe any significant aggregation.

As can be seen from Figure 5, at relatively low POSS content such as 0.09 mol %, almost no significant aggregated particle of POSS were observed [Fig. 5(a)]. However, at relatively high POSS concentration such as 0.48 mol %, only very small amount of aggregated particles of POSS was found. Significant aggregation was found and the particle diameter is about 10–20 nm when POSS concentration reached 0.84 mol % [Fig. 5(b)] and the aggregated particle showed a further aggrandizement tendency with an increase in the POSS concentration, such as 1.36 mol %, in the blend [Fig. 5(c)]. The results are in good agreement with those of XRD, further confirming

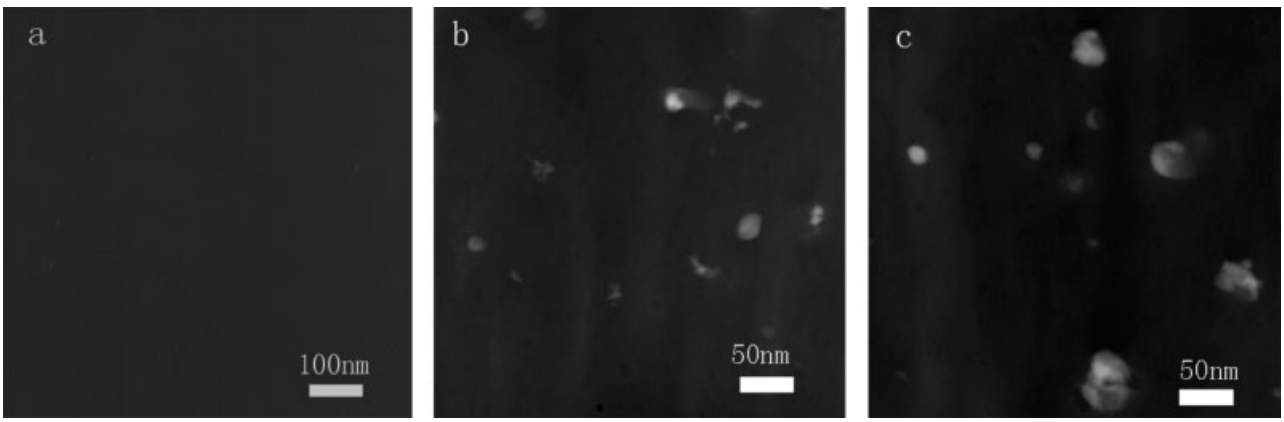

Figure 5 TEM micrographs of PAS-POSS blends with three different POSS molar content: (a) 0.09, (b) 0.84, and (c) 1.36 mol %.

that at the relatively high POSS content, POSS aggregation happens and the aggregation effect increases with the POSS concentration increasing.

In addition, we found that the films formed from PAS-POSS blends were transparent when the POSS content is below 1.36 mol % (5.10 wt %), indicating that the POSS nanoparticles have good molecular miscibility in the hybrid nanocomposites at a relatively low POSS content. However, the PS-POSS films were hazy when the POSS content is even at 0.09 mol % content (0.54 wt %), which is attributed to strong aggregation effect of the POSS molecules owing to the poor interaction between POSS and PS molecules. It is consistent with the results of the XRD and TEM.

FTIR analysis

To further reveal the T_g change mechanism involved in the PAS-POSS blends, the characterization of their FTIR spectra ranging from 1150 to 1075 cm^{-1} for the pure POSS and various PAS-POSS blends is shown in Figure 6. It is seen that the characteristic vibration peak centered at 1109 cm^{-1}, which is assigned to Si—O—Si band of POSS cages, shifts toward lower frequency in the hybrid system when a very small amount of POSS was mixed with the PAS. When the POSS contents further increase, the maximum absorption peak of Si—O—Si shifts slightly toward higher frequency gradually and further shifts toward to higher wavenumber with the increase in POSS content. For instance, the Si—O—Si maximum absorption peak of POSS at 1109 cm^{-1} decreases to 1107 cm^{-1} in the PAS-POSS 0.09%, but increases to 1108 cm^{-1} in the PAS-POSS 0.48% and 1109 cm^{-1} for PAS-POSS 0.84%.

Similar phenomenon also was found in expanded FTIR spectra from 1800 to 1675 cm^{-1} for the pure PAS and various PAS-POSS blends (Fig. 7). The mother PAS shows a characteristic carbonyl

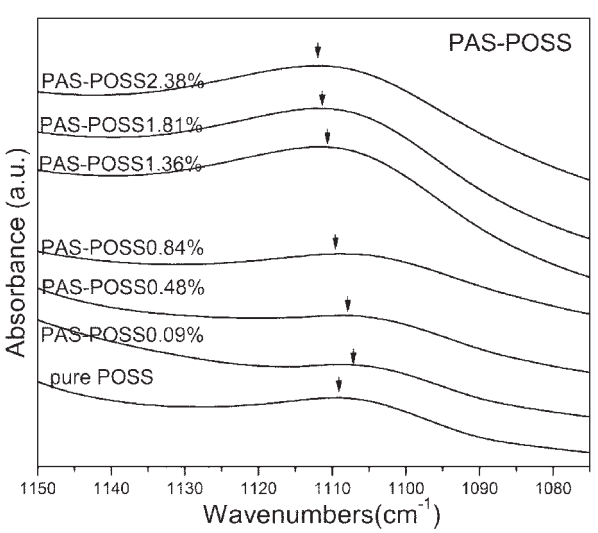

Figure 6 Expanded FTIR spectra ranging from 1150 to 1075 cm^{-1} for POSS and PAS-POSS blends.

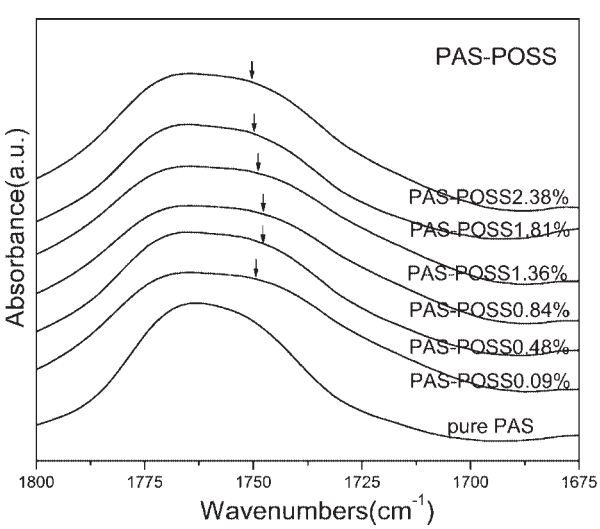

Figure 7 Expanded FTIR spectra ranging from 1800 to 1675 cm^{-1} for PAS and PAS-POSS blends.

vibration band centered at 1763 cm^{-1}. When the POSS moiety is mixed into the PAS, the vibration band is obviously broadened asymmetrically in the high-frequency region, and a significant absorption shoulder peak appears in the low-wavenumber region ($\sim$ 1750 cm^{-1}). The enhancement of absorption band in high-wavenumber region may be originated from the strong dipole–dipole interaction between POSS and PAS. The new absorption shoulder peak in low-wavenumber region mainly results from the dilute effect, which first shifts toward lower wavenumber, then shifts toward higher wavenumber with the increase in POSS content owing to the POSS aggregation. This is consistent with the change of Si—O—Si characteristic vibration peak of POSS in Figure 6.

Because of the absence of the dipolar carbonyl group in the structure of PS, the characteristic vibration peak of Si—O—Si has no obvious change in the PS-POSS blends, showing that almost no significant dipole–dipole interaction between POSS and PS molecules exists in PS-POSS blends.

Cheam studied the relationship between the dipole interaction potential (V_{dd}) and the FTIR vibration frequency shift (Δv_i), which is expressed as follows:[32]

$$\Delta \upsilon_i = \frac{V_{dd}}{hc} \quad (1)$$

where h is Planck's constant and c is the velocity of light. The frequency shift of characteristic vibration absorption is much related to the strength change of dipole interaction of characteristic vibration band with surrounding other polar group. The absorbance frequency will increase with the enhancement of dipole interaction and decrease with the weakening of dipole interaction. Painter studied the interaction potential between two dipoles, A and B, which is expressed in the following formula:[33]

$$V_{dd} = -\mu_A \mu_B [\hat{e_A}\hat{e_B} - 3(\hat{e_A} \bullet r_{AB})(\hat{e_A} - r_{AB})]/r_{AB}^3 \quad (2)$$

where μ is the value of dipole moment and $\hat{e}$ is a unit vector describing the direction of the dipole moment and r_{AB} is the distance between the centers of the dipoles. From formula 2, it is known that the increase of the distance between the centers of the dipoles will lead to the drop of the dipole interaction. Based on the theory and the FTIR spectra, the T_g change of the POSS-containing hybrid nanocomposites can be well explained. When the POSS is mixed into the PS matrix, owing to the absence of strong dipole–dipole interaction between POSS and PS, the POSS significantly enlarges the distance between PS molecule chains and mainly plays a diluent role. The dilution effect is much larger than the hindrance of homopolymer molecular chain motion from nanosized POSS that provides positive contribution to T_g increase. Therefore, the T_g in PS-POSS hybrid nanocomposites always decreases even at very low POSS content. Correspondingly, when a very small amount of POSS (0.09 mol %) is mixed uniformly into PAS matrix, POSS similarly plays a diluent role due to enlarging the distance between dipolar carbonyl group of PAS homopolymer molecular chains and decreasing the dipole–dipole interaction between parent polymers. However, at the same time, the new strong interaction between dipolar carbonyl group of PAS and POSS and hindrance effect of molecular chain motion from nanometer size POSS plays main role to result in T_g increase in PAS-POSS blends. The strong dipole interaction increases with POSS content when POSS nanoparticles are uniformly mixed into the PAS matrix. When the POSS content further increases, the dipole–dipole interaction between PAS and POSS decreases owing to the POSS aggregation. This is the main reason that T_g value of PAS-POSS blends shows a tendency of first increasing, then decreasing with the increase in the POSS content. Therefore, when the POSS content reaches 0.48 mol %, the new strong interaction between dipolar carbonyl group of PAS and POSS reaches maximum, then decrease at higher POSS content due to the physical aggregation of the nanosized POSS. It is consistent with the results of DSC and is further confirmed by FTIR, XRD, and TEM.

CONCLUSIONS

PAS-POSS and PS-POSS blends containing various POSS contents were prepared by the solution-blending method and characterized by FTIR, XRD, and TEM spectra. Their thermal properties were evaluated by DSC and TGA, and change mechanism of thermal properties of POSS-containing hybrid nanocomposites is investigated by FTIR, XRD, and TEM. The results show that POSS can effectively improve the thermal stability of the PAS-POSS blends at low POSS content, which is mainly assigned to strong dipole–dipole interaction between POSS and polymer, and the hindrance of homopolymer molecular chain motion from nanosized POSS. At relatively high POSS content, T_g value of PAS-POSS blends decreases with the increase in POSS content, which is attributed to the POSS aggregation. On the contrary, in the PS-POSS blends, T_g always decreases even at very low POSS content, which is due to the weak dipole–dipole interaction between the POSS and PS molecules. Simultaneously, it is also found that the dispersion of nanometer POSS in the hybrid nanocomposites is also one of the key factors affecting the thermal properties of nanocomposites.

However, the heat degradation temperature is always remarkably enhanced at low POSS content in these hybrid nanocomposites, which provides an important potential application as flame retardant for these hybrid nanocomposites.

References

1. Lee, K. M.; Han, C. D. Polymer 2003, 44, 4573.
2. Fina, A.; Tabuani, D.; Frache, A.; Camino, G. Polymer 2005, 46, 7855.
3. Zhao, Y.; Schiraldi, D. A. Polymer 2005, 46, 11640.
4. Fu, B. X.; Yang, L.; Somani, R. H.; Zong, S. X.; Hsiao, B. S.; Phillips, S.; Blanski, R.; Ruth, P. J Polym Sci B: Polym Phys 2001, 39, 2727.
5. Fu, B. X.; Gelfer, M. Y.; Hsiao, B. S.; Phillips, S.; Viers, B.; Blanski, R.; Ruth, P. Polymer 2003, 44, 1499.
6. Shen, Z.; Cheng, Y. B.; Simon, G. P. Macromolecules 2005, 38, 1744.
7. Rawal, A.; Urman, K.; Otaigbe, J. U.; Schmidt-Rohr, K. Chem Mater 2006, 18, 6333.
8. Beek, W. J. E.; Wienk, M. M.; Kemerink, M.; Yang, X.; Janssen, R. A. J. J Phys Chem B 2005, 109, 9505.
9. Quist, P. A. C.; Beek, W. J. E.; Wienk, M. M.; Janssen, R. A. J.; Savenije, T. J.; Siebbeles, L. D. A. J Phys Chem B 2006, 110, 10315.
10. Wang, L.; Liu, Y.; Jiang, X.; Qin, D.; Cao, Y. J Phys Chem C 2007, 111, 9538.
11. Baney, R. H.; Itoh, M.; Sakakibara, A.; Suzuki, T. Chem Rev 1995, 95, 1409.
12. Carroll, J. B.; Waddon, A. J.; Nakade, H.; Rotello, V. M. Macromolecules 2003, 36, 6289.
13. Liang, K.; Li, G.; Toghiani, H.; Koo, J. H.; Pittman, C. U., Jr. Chem Mater 2006, 18, 301.
14. Zhang, H.; Kulkarni, S.; Wunder, S. L. J Phys Chem B 2007, 111, 3583.
15. Huang, C. F.; Kuo, S. W.; Lin, F. J.; Huang, W. J.; Wang, C. F.; Chen, W. Y.; Chang, F. C. Macromolecules 2006, 39, 300.
16. Zheng, L.; Hong, S.; Cardoen, G.; Burgaz, E.; Gido, S. P.; Coughlin, E. B. Macromolecules 2004, 37, 8606.
17. Hao, N.; Bohning, M.; Goering, H.; Schonhals, A. Macromolecules 2007, 40, 2955.
18. Kang, J. M.; Cho, H. J.; Lee, J.; Lee, J. I.; Lee, S. K.; Cho, N. S.; Hwang, D. H.; Shim, H. K. Macromolecules 2006, 39, 4999.
19. Iyer, S.; Schiraldi, D. A. Macromolecules 2007, 40, 4942.
20. Kopesky, E. T.; Haddad, T. S.; Cohen, R. E.; Mckinley, G. H. Macromolecules 2004, 37, 8992.
21. Soong, S. Y.; Cohen, R. E.; Boyce, M. C.; Mulliken, A. D. Macromolecules 2006, 39, 2900.
22. Kopesky, E. T.; Haddad, T. S.; Mckinley, G. H.; Cohen, R. E. Polymer 2005, 46, 4743.
23. Kopesky, E. T.; Mckinley, G. H.; Cohen, R. E. Polymer 2006, 47, 299.
24. Baldi, F.; Bignotti, F.; Fina, A.; Tabuani, D.; Riccò, T. J Appl Polym Sci 2007, 105, 935.
25. Carroll, J. B.; Frankamp, B. L.; Rotello, V. M. Chem Commun 2002, 1892.
26. Naka, K.; Itoh, H.; Chujo, Y. Nano Lett 2002, 2, 1183.
27. Feng, Y.; Jia, Y.; Xu, H. J Appl Polym Sci 2009, 111, 2684.
28. Harrison, P. G.; Hall, C.; Kannengiesser, R. Main Group Met Chem 1997, 20, 515.
29. Xu, H. Y.; Kuo, S. W.; Lee, J. S.; Chang, F. C. Macromolecules 2002, 35, 8788.
30. Xu, H. Y.; Yang, B. H.; Wang, J. F.; Guang, S. Y.; Li, C. Macromolecules 2005, 38, 10455.
31. Yang, B. H.; Li, H. Y.; Wang, J. F.; Gang, S. Y.; Li, C. J Appl Polym Sci 2007, 106, 320.
32. Cheam, T. C.; Krimm, S. Chem Phys Lett 1984, 107, 613.
33. Painter, P. C.; Pehlert, G. J.; Hu, Y.; Coleman, M. M. Macromolecules 1999, 32, 2055.